Int. J. Metrol. Qual. Eng. 14, 9 (2023)

https://doi.org/10.1051/ijmqe/2023004

International Journal of Metrology and Quality Engineering

Available online at:
www.metrology-journal.org

SHORT COMMUNICATION OPEN ACCESS

First study on harvesting electromagnetic noise energy generated by the frequency converters

Mohamed Haythem Raouadi[1,*], Jean Pierre Fanton[2], and Oualid Touayar[3]

[1] AEA Unity, CRTEn, Technopole of BorjCedria BP. 95, 2050 Hammam'Lif Tunisia
[2] ECAM-EPMI, Cergy-Pontoise, France
[3] Materials, Measurements and Applications Research Laboratory, Département de Génie Physique et Instrumentation, National Institute of Applied Sciences and Technology, INSAT, University of Carthage BP676, 1080 Tunis Cedex, Tunisia

Received: 24 September 2021 / Accepted: 9 April 2023

Abstract. This paper proposes a novel environmental energy harvesting process. The source of energy consists of the electromagnetic (EM) noise emitted by the frequency converter system (inverter) and the harvester is composed by a monopole antenna and a full rectifier circuit. The operation of the frequency converter using MOSFET and IGBT switchers produces parasite currents in high frequency (100 KHz to 30 MHz) which are the principal cause of radiated EM noise. We have demonstrated that we can convert this EM noise into useful electrical energy to power wireless sensor nodes (WSNs) and other electronic devices. Experimentally, the EM noise is produced when the system "frequency converter + charge" is in operation mode. Moreover, the harvester has produced an uninterrupted power of 40 mW measured in accredited ISO/IEC 17025 laboratory. Furthermore, we have presented the output power of our device stored in 1 μF capacitor with demonstration examples of loading charges. These results offer opportunities for self-powered WSNs and electronic devices on a very large area of industrial applications with less use of conventional batteries.

Keywords: Frequency converter systems / EM noise harvesting energy / self-powered devices

1 Introduction

Micro-energy harvesting technique is a process wherein the environment sources such as wind flow, sun radiation, vibrations, temperature gradients, light, etc., are converted using the same active sensing process to obtain small levels of output currents or voltage and then the resulting power will be in the range of μW to mW. Major benefits include battery-less operation, exploiting free ambient energy, enabling otherwise impossible applications like permanently inserted sensors inside building walls and human body, etc. But still the major inconvenient of these alternative sources is the interruption of power generation due to the interruption of the source of energy (very low velocity of wind, no vibration, no sun, light off, constant temperature, etc.) [1–11].

In the same context, researchers have studied the harvesting of radiated electromagnetic (EM) energy contained in radio frequency (RF) signals from RF transmitters like Wi-Fi routers, TV towers, Cellular stations, Satellite transmitters, FM or AM Radio transmitters and more. The major advantage of this technique is the no-interruption of the energy source. In fact, it has been found that radiated electromagnetic radio frequency energy (EM-RF) harvesting can be one of promising alternatives to obtain energy to power wireless sensors without dependence on environmental parameters like wind flow, temperature gradient, sun, etc. [12–19]. In this direction, researchers have developed the radiated EM-RF energy harvesting systems, which are composed by antenna, impedance matching circuit, rectifier, and the energy storage device or load [20–25]. Also, many works have been then focused on the improvement of the EM-RF output harvester systems [26–28]. The results are very promising but still the major inconvenient is that the output power of this technique does not exceed hundreds of μWatts because their sources of energy are relatively low (Wi-Fi emission, telecommunication station, radio emission station, satellite transmission, etc.) [29–33].

The novelty of this work is the valorization of another ambient radiated EM energy much more powerful than the radiated EM-RF energy which is the EM noise produced by the frequency control of the electrical power converters (inverters). In fact, frequency power converters are the components that permit the conversion between ac and dc power systems in both ways using frequency control technique such as Pulse Width Modulation (PWM) and IGBT-MOSFET switchers, inducing a very important EM

* Corresponding author: med_haythem@hotmail.fr

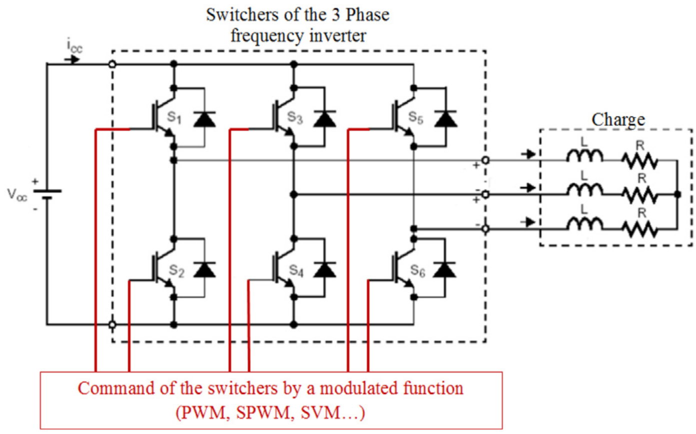

Fig. 1. Electric schema of 3 phases frequency converter.

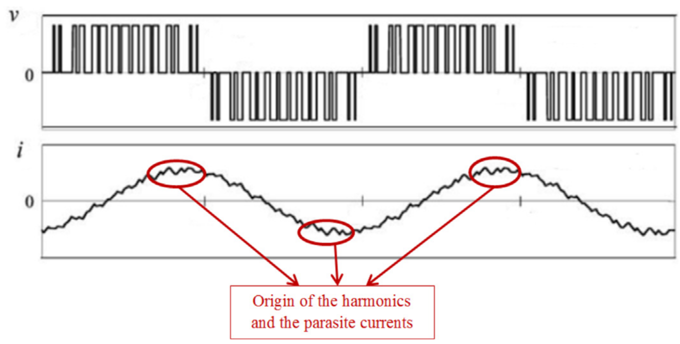

Fig. 2. Output voltage and current from one phase of the frequency converter.

Noise energy related to the common-mode and differential mode current [34]. This radiated EM noise has been studied in the field of Electromagnetic Compatibility (EMC). Researchers and engineers have developed different filtering and shielding techniques neutralizing the emission of EM noise in the high frequency level to avoid interference with other electronic devices [35]. In fact, these studies ware focused on the elimination of the produced EM noise from 30MHz to few GHz [36]. Thereby, we have focused in our study on the valorization of this radiated EM noise under 30MHz. Therefore, we have showed in this paper the first results proving the effectiveness of this energy source to power many electronic devices such as the wireless sensors, actuators and also other electronic devices in aim to minimize the use of batteries. The experiment and measurements highlighting this approach is conducted in an ISO/IEC 17025 accredited laboratory. The antenna will be the transducer that captures the EM noise energy followed by the rectifier circuit which produces a continuous voltage. In the following, the different stages of this process will be described as well as a discussion of obtained results and potential applications will be presented.

2 Frequency converter systems outputs and em noise enhancement factors

2.1 Frequency power converter system

The main frequency converter structures that can be found are:

– AC-DC or DC-DC power supply, their power are from 10 W to a few kW, the operating frequency is between 10 Hz and 100 kHz.
– Voltage inverter, they are used for actuators electric or in combination with generators for generating AC voltage. Their power are from a few kW to a few hundred kW, the switching frequencies are in the range from 10 to 20 kHz. In this type of configuration, the converter can be distant from the charges by several tens of meters.

All frequency converter systems use semiconductor switchers which are driven by various modulation techniques (pulse width modulation PWM, space vector modulation SVM, etc.) [37]. So, the main switch is controlled by modulation function which modulates the power transfer to the charge (Fig. 1).

Figure 2 shows the output voltage and current of one phase of the frequency converter presented in Figure 1. We can see that the voltage output v is the result of the switches controlled in opening and closing by modulation functions (Fig. 1). The form of the current i is the result of the smoothing performed by the charge. Hence, the real waveforms of the converters outputs voltages and currents are non-sinusoidal and contain harmonics. These harmonics will be at the origin of high frequency parasite currents and EM noise [38,39].

Thus, the search for miniaturization of the converter devices has led to the development of semiconductors whose frequency of work has not stopped to increase:

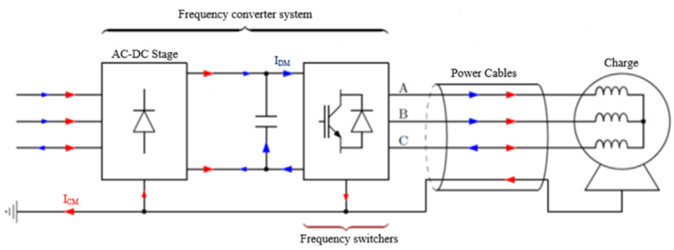

Fig. 3. Differential mode I_{DM} and common mode currents I_{CM} through different stages of the frequency converters.

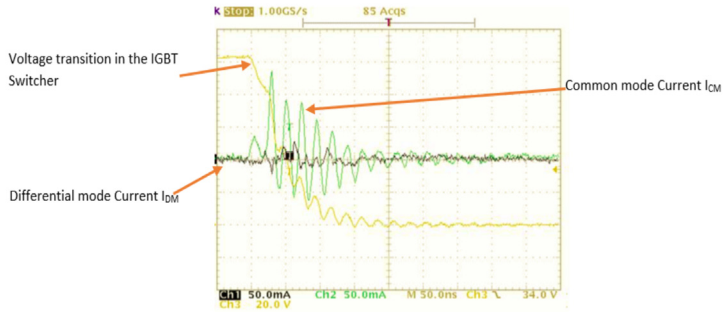

Fig. 4. Correlation between switched voltage in yellow, the common mode current I_{CM} in green and the differential mode current I_{DM} in black [43].

currently a DC-AC power supply operates at 500 kHz whereas 10 years ago the frequency was more like 20–50 kHz. This trend continues and we see advertisement for devices switching at 3 MHz. This evolution has been made possible through better process control technologies for manufacturing power components and innovative topologies (COOLMOS, IGBT Trench, etc.) and the use of different materials such as Sic [40].

2.2 Diversity of areas of use

The areas of applications where inverters are used multiplied during the last three decades. We passed of applications limited to the field of railway traction (thyristors, GTO) and variable speed drives in industrial environment (bipolar transistor and diode inverter fast feeding synchronous and/or asynchronous motors) or induction heating to applications generalized in the field of transport: automobile, aeronautics, home automation, personal computing, fluorescent and now LED lighting and renewable energy. Evolution technological has selected components with an insulated grid, easy to control and having either conduction through electric field (MOSFET) or conduction by field and by diffusion (IGBT). They also are used in high voltage in reducing switching times. The use of these components allowed a strong increase in frequencies switch allowing miniaturization of devices static conversion, thus promoting their use. Similarly, the reduction in switching times has allowed reduction of losses, also favoring reduction volume. However, these advantages find their limitation in the strong EMC constraints that they cause [40,41].

2.3 Origin of current parasite generation

Frequency power converter systems (inverts) is based on the principle of the switching cell: it is the association of two switches that allow energy management between an input voltage source and a current source of outlet. So, to reduce losses during the switching process, it is necessary that the switchers of the frequency converter be very fast. Currently, the order of size of the switching gradients is around 100 at 1000 A/µs for dI/dt and from 5 to 50 kV/µs for dV/dt. According to the literature, these switching process produce two type of parasite currents: the differential mode current I_{DM} and the common mode current I_{CM} (Fig. 3). Researchers have proved that the common mode current I_{CM} is the principal source of the high frequency parasite currents and not the differential mode current I_{DM} [42]. In fact, Aime et al. [43] showed in Figure 4, as a result of switched voltage in yellow color in IGBT switcher, the production of common mode current I_{CM} equal at 130 mA in green color for a switching time equal at 300 ns and the production of differential mode current I_{DM} did not exceed 10 mA in black color. This current will be the main origin of EM noise radiation presented in Section 2.4.

2.4 Source of radiated EM noise

A radiated electromagnetic noise comes from one or both of the following processes:

– The alternating current flowing in a loop generates a magnetic field oscillating near the loop. When the magnetic field propagates away from the source, the energy turns into an electromagnetic wave with an electric field perpendicular to the magnetic field.

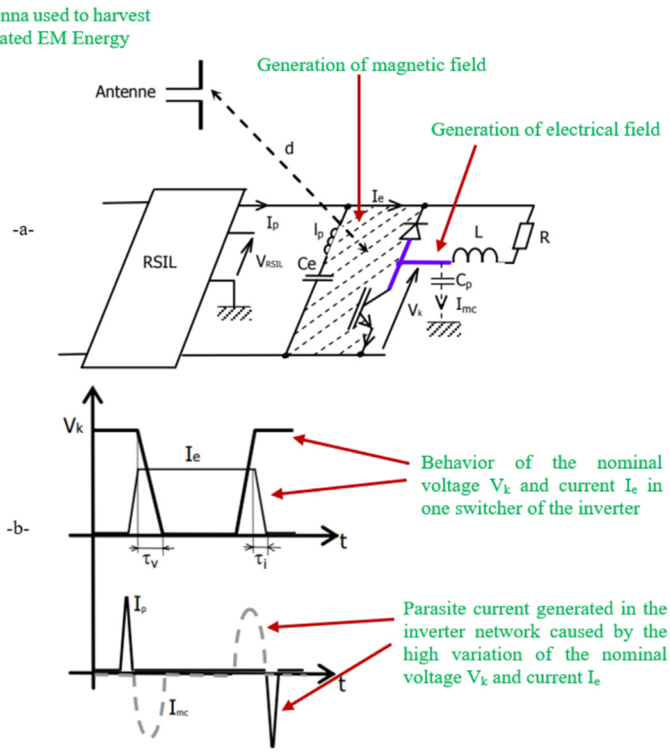

Fig. 5. Origin and coupling mode of disturbances electromagnetic of a static converter: (a) generation of radiated EM energy from magnetic and electric coupling; (b) parasite current produced by the high frequency switching [42].

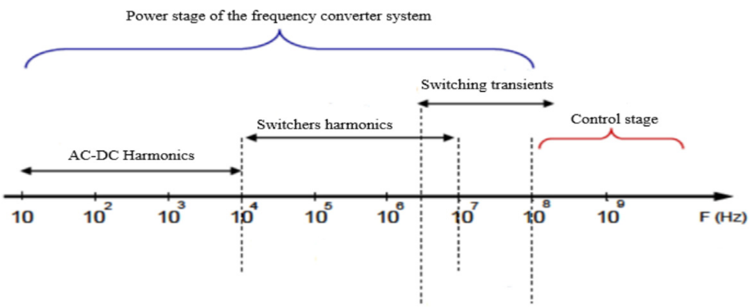

Fig. 6. Spectrum of EM noise radiation of the frequency converter [42].

– The alternating voltage appearing on a conductor generates an electric field oscillating near the conductor. The field is mainly electric, but as the distance from the conductor increases, the electric field propagates away from the conductor and the energy is transformed into electromagnetic wave. Part of the electrical energy is converted into a field magnetic perpendicular to the electric field.

By way of illustration, Figure 5 shows these phenomena in one switcher of the frequency converter connected to a stabilizing network line impedance (RSIL) and in a charge modelized by resistance R and inductance L: in the mesh surrounding the hatched area, the current I_e undergoes very rapid variations in high frequency; the loop thus formed is similar to a magnetic radiating dipole (Fig. 5a). In addition, the conductors shown in blue are subject to strong variations in voltage V_k, they constitute an electric radiant dipole and can transmit to earth impulse currents I_{CM} via stray capacitance symbolized by C_p between the device and the earth (Fig. 5a). Thus, these high frequency variations in the nominal current I_e and nominal voltage V_k produce an important current parasite which is the principal source of EM noise radiated energy (Fig. 5b).

Therefore, frequency power converter systems contain elements capable of behaving like transmitting antennas such as AC-DC converter stage, control stage, switchers-fan stage (Fig. 6). In addition, these elements can unintentionally transfer energy through electrical/magnetic circuits (near field coupling) or electromagnetic waves (far field coupling) and the sources interfere with each other giving rise to complex effects of inter-modulation [42–50]. So, we can exploit the radiated EM noise energy of the inverters to valorize it in powering small electronic devices.

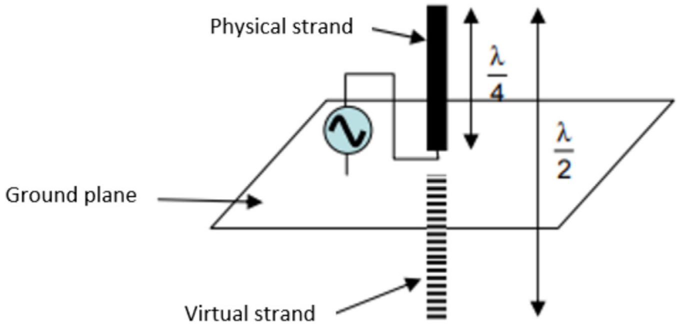

Fig. 7. Monopole antenna.

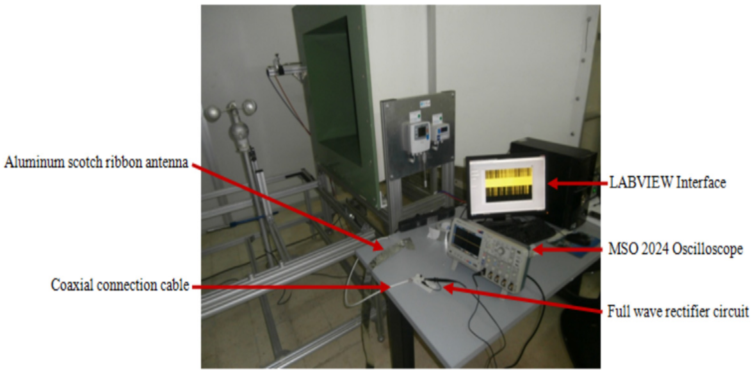

Fig. 8. Used measuring system in the wind tunnel composed by the oscilloscope, LABVIEW interface, the antenna and the electronic circuit.

2.5 EM noise harvester design

For EM noise harvesting, different antennas (or rectennas) are used to capture electromagnetic signals emitted from sources like mobile phones or radio stations, which are then used to power small electronic systems [51,52]. In our case, the main radiated EM noise is produced by the common mode current I_{CM} of the inverter [53]. The frequency of this EM radiation varies from 1 MHz to 10 MHz (Fig. 6) which implies EM waves with wavelength from 300 m to 30 m.

For our first study, we chose to harvest this EM noise using a monopole antenna which is one half of a dipole antenna. In fact, a dipole antenna has two halves, while a monopole model replaces one of the halves with an electrically conductive surface known as the ground plane, which behaves like the other half of a dipole antenna (Fig. 7). With a large enough ground plane, the monopole antenna can be as strong as the dipole antenna [54].

Therefore, the first pole of our developed antenna is an aluminum scotch ribbon, and the second pole is the ground. The use of the metal scotch ribbon has several advantages: very cheap, can be installed in different ways and geometry, very discreet, heat and humidity resistant and not bulky. This antenna will be related to a full-wave rectifier circuit RB142 and a charging capacity by a regular TV coaxial cable (Fig. 8 and video M1, M2 and M3).

2.6 Experimental study

The experimental study was done in an accredited ISO/CEI 17025 v2017 wind tunnel laboratory made for anemometer calibration [33]. The choice of this laboratory was done to be sure that the installation of the converter and the charge respects the EMC standards and the EM noise produced will be optimal. This wind tunnel is equipped with a 30 kW three phase motor controlled by Sinus-K Santerno frequency converter. The nominal current and voltage of this system is 30 A and 100 Volts by phase. Figure 9 explain the process of our EM noise harvester: the EM noise produced by the whole system of the inverter and the charge will produce the EM noise which will be captured by the antenna and transformed to DC output using the rectifier circuit.

To study the signal of our EM harvester, we have used the oscilloscope MSO2024 and the output signal is displayed in the oscilloscope and in the PC in the same time. Thus, the EM noise will be harvested by our antenna and the full-wave rectifier will deliver a continuous voltage signal as long as the motor controlled by the frequency converter is running even at very low speed (video M1, M2 and M3).

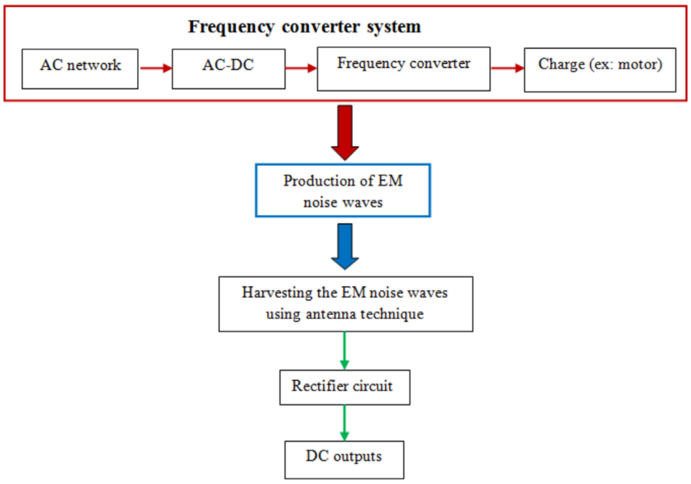

Fig. 9. EM noise energy harvesting process.

2.7 Characteristic of the received Signal

We, first, have studied the characteristics of the signal delivered by the antenna based on aluminum scotch ribbon with 10 m length and measured across a resistor of 10 kΩ (Fig. 10a).

Figures 10b and 10c illustrate the shape of the signals obtained using LABVIEW interface (video M1). The measurements of the output signal are, considering the average of the peaks (Fig. 10b), 16 Volts which means 1.6 mA current and 25 mW output power.

We underline that the shape of the measured signal is very similar to the shape of the signal of the common mode current I_{CM} presented on Figure 4 thus showing that the noise EM collected by the antenna is no other than the image of the transient I_{CM} current generated by the frequency converter switches and characterized by decreasing peaks after 10 µs.

3 Results

3.1 Energy storage

In a second step, we have studied the output signal (Fig. 12) of the antenna with the full-wave rectifier circuit (Fig. 11). We notice that the full wave rectifier circuit eliminates the negative part of the signal seen in Figure 10b. For more illustration we add to our developed EM noise harvester a white LED. We clearly observe the light of the white diode (Fig. 13 and video M2).

This charge generated from EM noise can be stored in a load capacitor C_{L} using the full-wave rectifier circuit (Fig. 14a). We have used a conventional full-wave rectifiers RB142 composed by 04 diodes *p-n* junction and 1 µF capacity. The energy loss of this type of rectifier is evaluated by 35% of the input energy from the antenna [51].

Thus, and during the positive signal two forward-biased diodes (D1 and D3) let the generated current flow through and charge C_{L}. The remaining two diodes (D2 and D4) are reversed-biased and block the current flow. During the negative signal the direction of the generated current is reversed, and C_{L} is charged through D2 and D4. Then, the voltage V_0 across C_{L} and the stored energy will increase. We assume the signal is periodic (Fig. 10b and video M3) and that the generated charge is always the same value of Q. Then, at each new cycle, Q is redistributed among C_{L}. Assuming ideal diodes (zero voltage drop when forward biased and no current under reverse bias) and no leakage current, at an arbitrary cycle N we get (Eqs. (1)–(4)):

$$Q + Q_L(N-1) = Q_L(N), \tag{1}$$

$$Q_L(N) = V_0(N) * C_L, \tag{2}$$

$$Q_L(N-1) = V_0(N-1) * C_L, \tag{3}$$

where Q is the charge delivered by the antenna and the rectifier circuit in one cycle, $Q_{\mathrm{L}}(N-1)$ is the charge harvested in the capacity C_{L} after $N-1$ cycles, $Q_{\mathrm{L}}(N)$ is the charge harvested in the capacity C_{L} after N, $V_0(N-1)$ is the voltage of the capacity C_{L} after $N-1$ cycles and $V_0(N)$ is the voltage of the capacity C_{L} after N cycles.

Then, we can have the relation between V_0 and Q in equation (4):

$$V_0(N) = N * Q/C_L. \tag{4}$$

Thus, larger values of C_{L} permit to store more energy. However lower values of C_{L} lead to a faster increase of V_0.

The charge generated from EM noise can be stored in a load capacitor C_{L} (Fig. 13 and Attached Movie M3). The stored energy in C_{L} is given by equation (5):

$$E_n = \frac{1}{2} C_L V_0^2(N), \tag{5}$$

where E_n the energy harvested in the capacity C_{L} after N cycles.

Figure 14b illustrates the obtained and measured DC voltage in the 1 µF capacitor C_{L}. The value of V_0 is about 20 Volts for 13 m antenna length, indicating an uninterrupted important power as long as the frequency converter

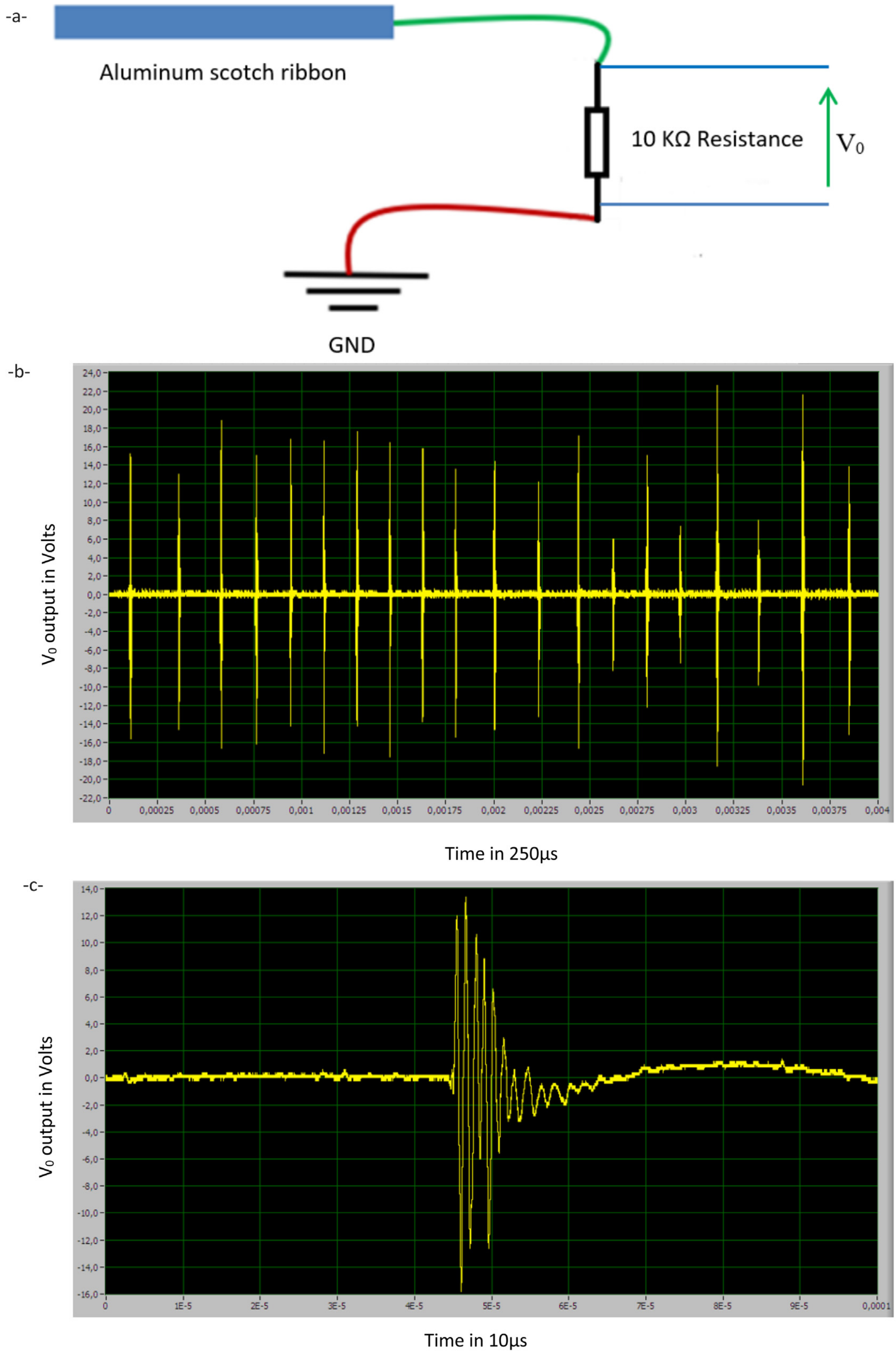

Fig. 10. (a) Circuit diagram, (b) signal output for 250 µs scale and (c) 10 µs scale.

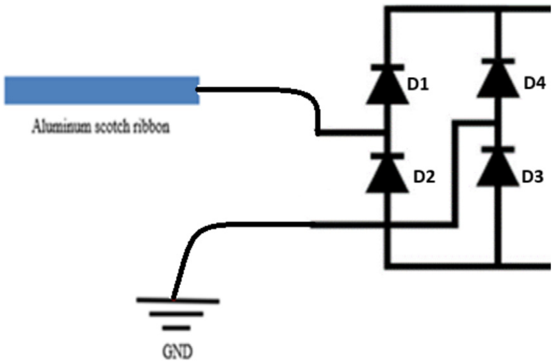

Fig. 11. Antenna connected to the full wave rectifier circuit.

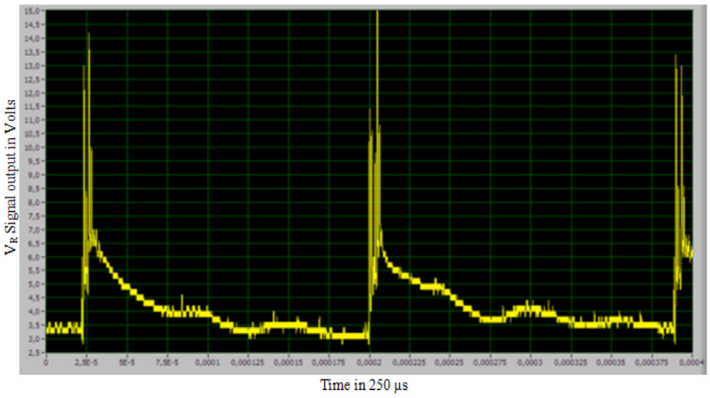

Fig. 12. Output of the developed EM noise harvester connected to the full rectifier circuit RB142.

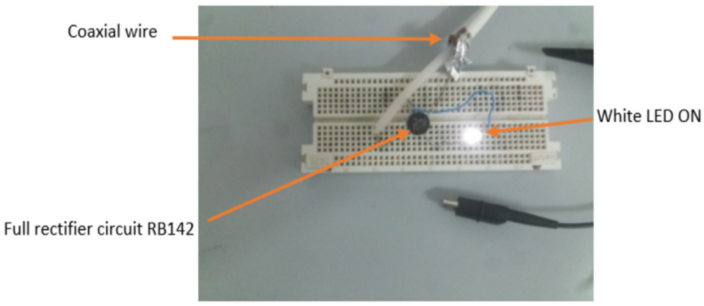

Fig. 13. Example of powering a white led diode with the antenna and the rectifier circuit RB142.

and the motor are in ON mode. For a more quantitative study we have used our developed EM noise harvester to evaluate the energy production of the antenna and its evolution as a function of the antenna length. Figure 15 shows an increasing of the stored energy when the antenna is much longer. We notice that from 13 m antenna length the power output is saturated. This result is explained by the fact that the frequencies of EM noise radiations produced by the used frequency converter system don't exceed 6 MHz. The shape of the obtained V_0 signal is quite similar to those obtained on previous works [22–44].

We have created an energy harvester that use EM noise energy generated by the frequency converter to serve as a source of electricity via scotch ribbon used as monopole antenna. Successfully, our energy harvester repeatedly generated electricity using the EM energy waves. The V_{max} was 20 Volts and the I_{max} was 4 mA. The output voltages are function of the length of the antenna (Fig. 15). In fact, to harvest the entire EM energy the antenna must have the length at least of $\lambda/10$ (λ is length of the EM wave) [48].

The effect of the distance from the source of the EM noise on the output of the harvester was also studied. In fact, the amount of energy that the EM harvester can

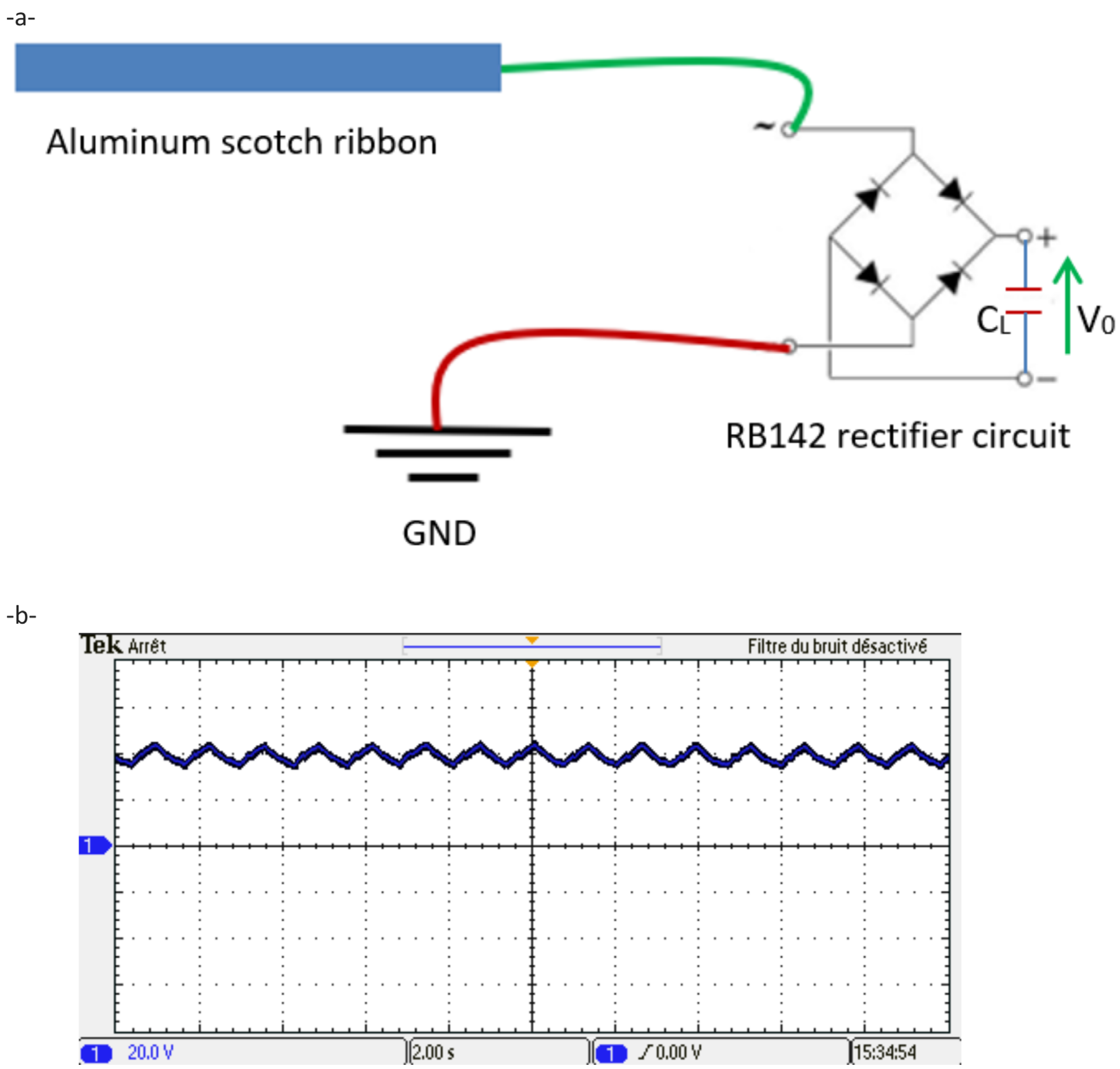

Fig. 14. (a) Our developed harvester with charging capacity C_L and (b) V_0 output of the 1 μF charging capacity for 13 m antenna length.

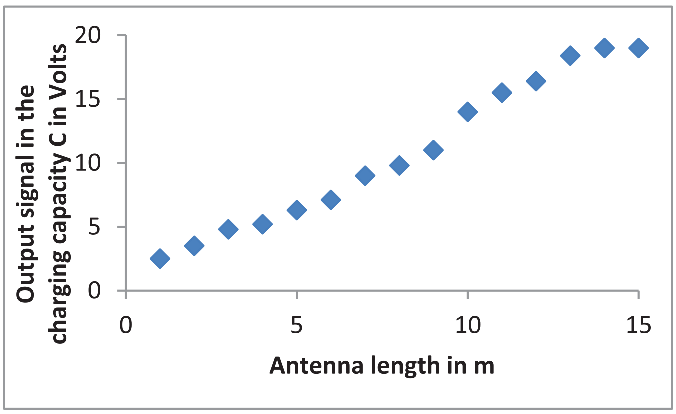

Fig. 15. Evolution of the output in the 1 μF charging capacity in function of the length of the antenna.

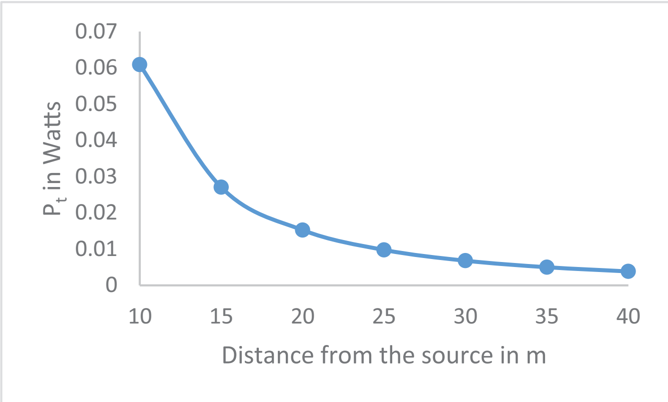

Fig. 16. Transmitted power P_t estimated with Friis equation function of the distance from the EM noise source.

Table 1. Comparison between different techniques used to power small electronic devices with our developed EM noise harvester.

Technique for micro energy harvesting	Maximum power output
Pyro-electric [42–55]	1.47 mW/cm^3
Piezo-electric [56]	5 mW/cm^3
RF-EM [44]	40 µW
Mechanical [51]	10 mW
Solar [51]	50 mW/cm^2
Micro turbine [51]	8 mW
Our developed EM noise harvester technique	40 mW

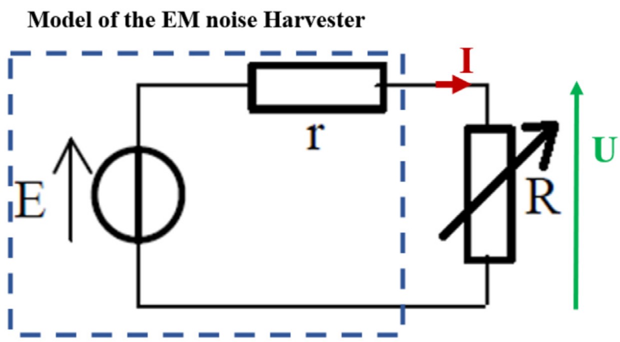

Fig. 17. The electronic model used to characterize the internal resistance r of our harvester.

receive is given by a combination of parameters including: the distance between the EM noise source and the energy harvester, the frequency of the EM noise, the power transmitted by the source of the EM noise. In our case, only the distance changes and the radiated EM received power can be estimated using the Friis equation (6) [34]. Thus, to have an efficient output, the harvester must be placed in a proximity of the EM noise source, and we can have an important radiated power sufficient to supply the wireless sensors, actuators and small electronic devices (Fig. 16).

$$P_r = \frac{P_t G_t G_r \lambda^2}{(4\pi R)^2}, \tag{6}$$

where P_r: power at the receiving antenna, P_t: output power from the source, G_t: gain of the transmitting source, G_r: gain of the receiving antenna, λ: wavelength = speed of light/frequency, R: distance between the harvester and the source of the EM noise.

On the other hand, we compare the output power of our harvester with output power of recently developed similar harvesters using other techniques based on small electronic devices such as pyroelectric, piezoelectric, photovoltaic, etc. (Tab. 1). We can see that harvesting EM energy noise from frequency converter systems is quite powerful compared to these techniques. Also, the power outputs depend on wind, sun, temperature variation, mechanical stress variation, etc. which area not continuous sources of power however the power source of our system is continuous when the frequency converter system is in ON mode. Moreover, our technique is very cheap, robust and easy to design and does not need a complex preparation like the pyro and piezoelectric films, the solar cells, the micro-wind turbines, etc.

3.2 Impedance characterization

Our harvester presented in Figure 14a can be modeled by a voltage generator with internal resistance. Thus, and to determine the internal resistance we have connected it to a varied resistor and the hole system can be presented in Figure 17 and its behavior in equation (7).

$$U = E - (R + r) * I, \tag{7}$$

where E is the voltage generator of the harvester, r is the internal resistance of the harvester, R is the varied load resistor, U the measured voltage of the resistor R and I is the current crossing the resistor R.

So, we have varied a load resistance R and we have measured the current and the voltage to deduce the value of the internal resistance and we found $r = 175\ \Omega$.

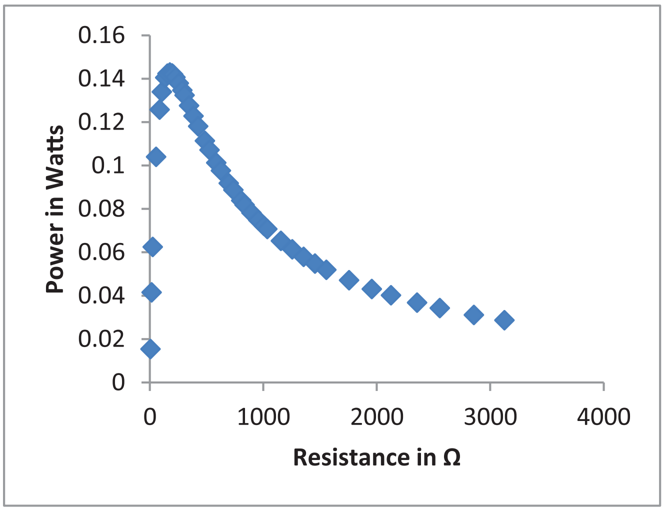

Fig. 18. The power generated by our EM harvester generator function of the resistance load.

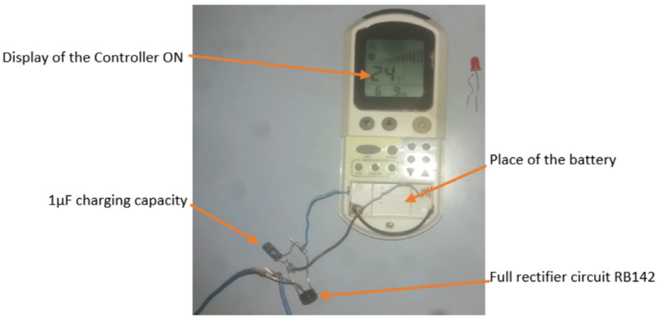

Fig. 19. Remote control powered by our EM harvester generator.

We then used the equations (8)–(10) to study and calculate the power transmitted from our generator to the load as a function of the value of the resistor load R (Fig. 18).

$$P = R * I^2, \tag{8}$$

$$P = \frac{E^2 * R}{(r + R)^2}, \tag{9}$$

$$P'(R) = \frac{E^2(r - R)}{(r + R)^3}, \tag{10}$$

where P is the transmitted power and P' is its derivative function.

It is thus determined that if the load has the same value as the internal resistance of the generator, the power dissipated by the load resistance R is maximum (Eq. (11) and Fig. 18).

$$P = \frac{E^2}{4 * R}. \tag{11}$$

We have verified the result presented in Figure 18 by powering a remote control of air conditioning with our EM noise harvester. In fact, the total resistance of the remote control is 1780 Ω and it needs 17 mW to work. So, we have used our EM harvester without impedance matching circuit and we can see the remote is ON (Fig. 19).

3.3 Metrology characterization

For the metrology characterization, we have studied the reproducibility of our measurements on a period of 5 days. We have, for that, calculated the average voltage of the capacity output named V_{CL} (Eq. (12)) and the experimental standard deviation S (Eq. (13)) from twenty values ($n = 20$). The results are grouped in Figure 20.

$$V_{CL} = \frac{1}{n}\sum_{i=1}^{n} V_{0_i}, \tag{12}$$

$$S = \sqrt{\frac{1}{n-1}\sum_{i=1}^{n}\left(V_{CL} - V_{0_i}\right)^2}. \tag{13}$$

Figures 20a and 20b present the evolution of the average measured signal delivered by the capacity C_{L} (1 μF) and its standard deviation S. It shows that there is constant energy on the period of 5 days for the same EM noise Harvester and depending on the length of the aluminum scotch ribbon. Figure 20c shows that the fraction S/V_{CL} doesn't exceed 10% value which considered as tolerance limit value for reproducibility considerations.

3.4 Example of applications

Our first measurements and experimental results prove that the EM noise harvester from the inverters can be an alternative source to the use batteries. In fact, potential applications of our developed EM noise harvester may interest the following areas (Fig. 21)

- Industrial application: an antenna composed by a metallic scotch ribbon or metallic paint and the ground can be placed without making a clutter and can be very discreet. This antenna will be related to the rectifier circuit to produce continuous voltage to power different electronic devices. Thus, the sensors used in industry (temperature, humidity, fire warning, etc.) can be directly powered by the EM noise harvesting system or this EM harvester will be the power source of rechargeable battery to avoid any power interruptions.
- Automotive application: frequency converters are very used in transport applications such as electric trains or electric cars to control their speed [44]. We can place the EM noise harvester without disturbing the other systems and the energy harvested can power electronic devices such as sensors and digital displayers. The antenna can be the same of the industrial application and its ground will be the chassis of the vehicle.
- Renewable energy: all renewable power stations use frequency converters to stabilize the voltage injected into the public network [57]. We can with simple way harvest

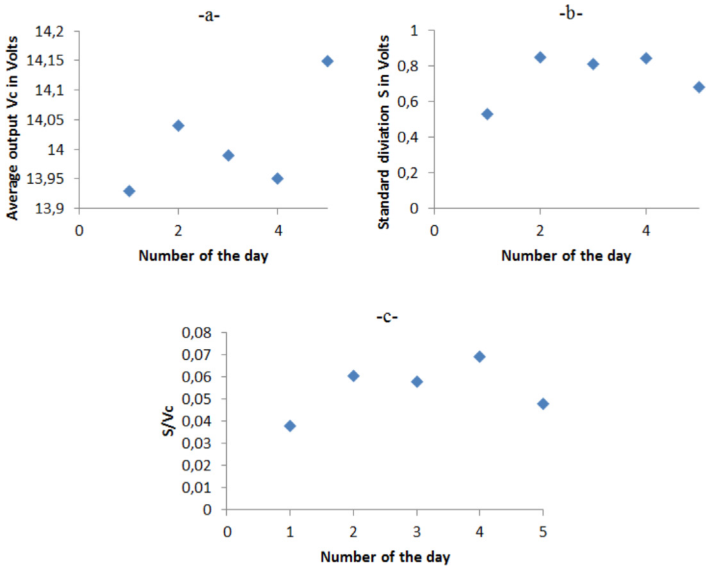

Fig. 20. (a) Average output V_C in Volts on 5 days, (b) standard deviation S of the measured signal V_C in 5 days and (c) the evolution of the fraction S/V_C on5 days.

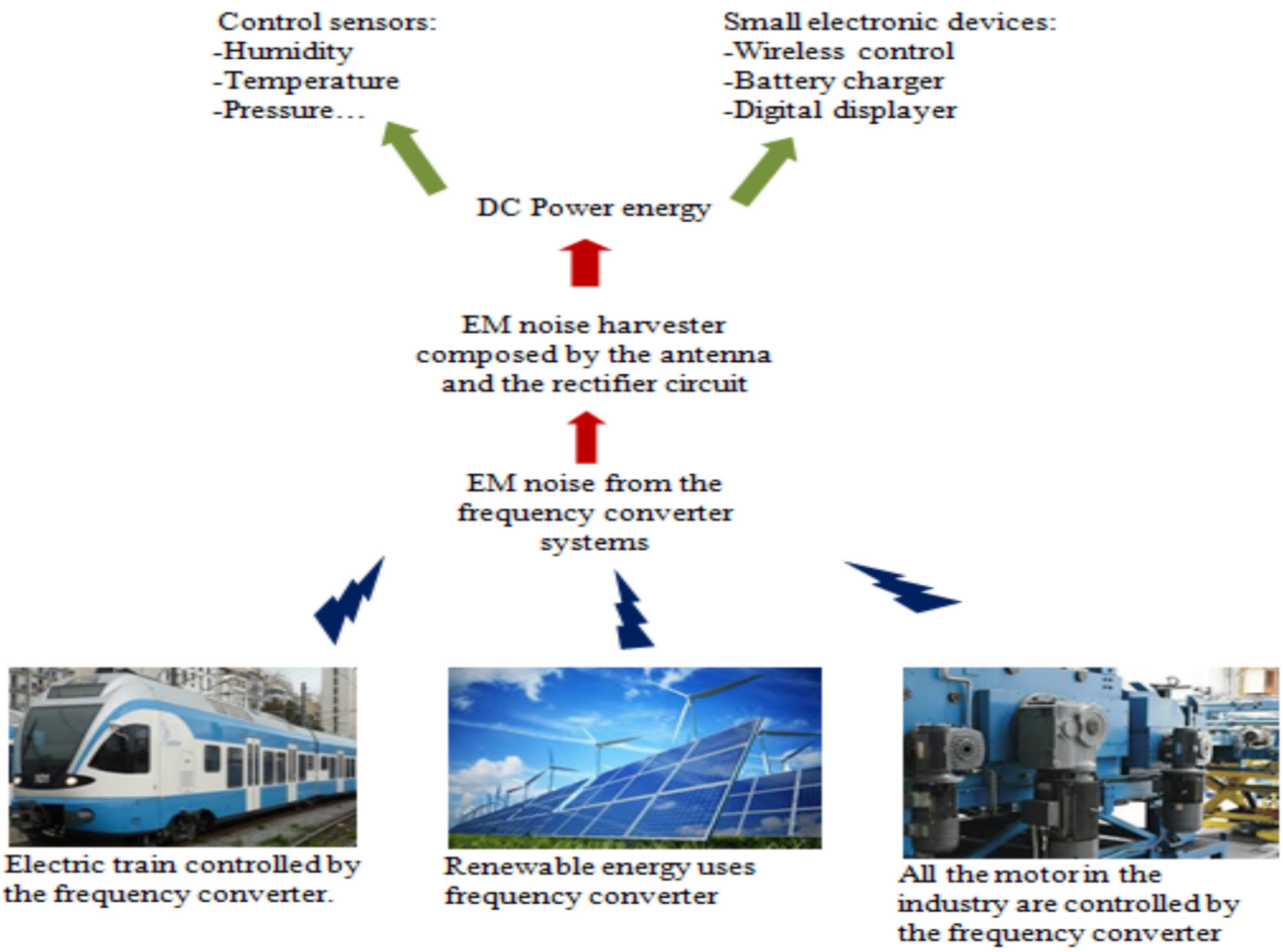

Fig. 21. Example of applications that can use our developed EM noise harvester.

the EM noise energy to have the wireless sensors of the smart grid, which send the data to the control stations, 100% renewable or use rechargeable battery powered by the EM noise harvester.

Another point is that if we use other developed rectifier circuit dedicated to micro-generators applications, we can increase the efficiency of the output energy by 30% [58]. Finally, next generation of frequency power converters will operate in much higher frequency (100 KHz) and the EM noise generated will be more powerful which will make EM noise harvester more efficient. It should also be noted that many industrial applications cannot meet the EMC standards and therefore the EM noise energy to harvest will be very important [59].

4 Conclusion

Different techniques of micro-energy harvesters can provide high pulsed energy output but the challenge to have a good time-average values of the outputs is still relevant. Therefore, most of these harvesters have difficulties for providing uninterrupted power and replace batteries for powering small electronic devices. In this paper, new measurements and experimental study had been done on the response of monopole antenna to the EM noise radiated by the frequency power converter systems. The antenna was based on commercial aluminum scotch ribbon and the measurements was done in accredited ISO/IEC 17025 wind tunnel. The experimental results and measurements show that the antenna output signal is the image of the parasite currents generated by the frequency converter system producing an uninterrupted current when the frequency converter of the wind tunnel is in operation. The produced power by our developed system was 40 mW which is good enough to power many sensors or electronic devices. The efficiency of our developed method was guaranteed by the ISO 17025 accreditation of the wind tunnel and its power converter system. We think that these results can be exploited in many industrial applications to develop inexpensive and efficient EM noise energy harvester based on metal scotch ribbon or metal. However, further research would be required to study the geometry effect of the antenna on the response of the EM noise harvester. Also, the presence of several frequency converters controlling machines in the same place have not been investigated; we estimate that in this case the EM noise will be very important and could increase further the current generated by the EM noise harvester.

Supplementary Material

The Supplementary Material is available at https://www.metrology-journal.org/10.1051/ijmqe/2023004/olm.

Video M1: The electromagnetic noise signal generated by the switchers of the inverter.

Video M2: Our developed electromagnetic noise harvester powring a white led.

Video M3: The output voltage across a capacity generated by Electromagnetic noise harvester system.

References

1. C. Hou, C. Li, X. Shan, C. Yang, R. Song, T. Xie, A broadband piezo-electromagnetic hybrid energy harvester under combined vortex-induced and base excitations, Mech. Syst. Signal Process. **171**, 108963 (2022)
2. A.G.A. Muthalif, M. Hafizh, J. Renno, M.R. Paurobally, A hybrid piezoelectric-electromagnetic energy harvester from vortex-induced vibrations in fluid-flow; the influence of boundary condition in tuning the harvester, Energy Convers. Manag. **256**, 115371 (2022)
3. J. Bjurström, F. Ohlsson, A. Vikerfors, C.Rusu, C. Johansson, Tunable spring balanced magnetic energy harvester for low frequencies and small displacements, Energy Convers. Manag. **259**, 115568 (2022)
4. C. Wang, S.-K. Lai, J.-M. Wang, J.-J. Feng, Y.-Q. Ni, An ultra-low-frequency, broadband and multi-stable tri-hybrid energy harvester for enabling the next-generation sustainable power, Appl. Energy **291**, 116825 (2021)
5. Q. Wen, X. He, Z. Lu, R. Streiter, T. Otto. A comprehensive review of miniatured wind energy harvesters, Nano Mater. Sci. **3**, 170–185 (2021)
6. K. Paul, A. Amann, S. Roy, Tapered nonlinear vibration energy harvester for powering Internet of Things, Appl. Energy **283**, 116267 (2021)
7. M. Kang, E.M. Yeatman, Coupling of piezo- and pyro-electric effects in miniature thermal energy harvesters, Appl. Energy **262**, 114496 (2020)
8. Z.-Y. Huo, D.-M. Lee, Y.-J. Kim, S.-W. Kim, Solar-induced hybrid energy harvesters for advanced oxidation water treatment, iScience **24**, 102808 (2021)
9. L. Battista, L. Mecozzi, S. Coppola, V. Vespini, S. Grilli, P. Ferraro, Graphene and carbon black nano-composite polymer absorbers for a pyro-electric solar energy harvesting device based on $LiNbO_3$ crystals, Appl. Energy **136**, 357–362 (2014)
10. R. Hamid, M. Rasit Yuce, A wearable energy harvester unit using piezoelectric-electromagnetic hybrid technique, Sens. Actuat. A **257**, 198–207 (2017)
11. Y. Wang, X. Liu, T. Chen, H. Wang, C. Zhu, H. Yu, L. Song, X. Pan, J. Mi, C. Lee, M. Xu, An underwater flag-like triboelectric nanogenerator for harvesting ocean current energy under extremely low velocity condition, Nano Energy **90**, 106503 (2021)
12. A.M. Baranov, S. Akbari, D. Spirjakin, A. Bragar, A. Karelin, Feasibility of RF energy harvesting for wireless GasSensorNodes, Sens. Actuat. ASNA 10692 (2018)
13. P. Nintanavongsa, U. Muncuk; D. Richard Lewis, K.R. Chowdhury, Wireless power transmission: state of the art and perspectives, Int. Rev. Electr. Eng. **14** (2019)
14. P. Nintanavongsa, U. Muncuk; D. Richard Lewis, K.R. Chowdhury, Design optimization and implementation for RF energy harvesting circuits, IEEE J. Emerg. Selected Top. Circ. Syst. **2** (2012)
15. M. Cansiz, D. Altinel b c, G. Karabulut Kurt, Efficiency in RF energy harvesting systems: a comprehensive review, Energy **174**, 292–309 (2019)
16. M. Grätzel, Solar energy conversion by dye-sensitized photovoltaic cells, Inorg. Chem. **44**, 6841–6851 (2005)

17. S. Wang, L. Lin, Z.L. Wang, Triboelectric nanogenerators as self-powered active sensors, Nano Energy **11**, 436–462 (2015)
18. G. Sebald, D. Guyomar, A. Agbossou, On thermoelectric and pyroelectric energy harvesting, Smart Mater. Struct. **18**, 125006 (2009)
19. M. Sharma, A. Chauhan, R. Vaish, V. Singh Chauhan, Finite element analysis on solar energy harvesting using ferroelectric polymer, Sol. Energy **115**, 722–732 (2015)
20. A. Bibo, M.F. Daqaq, Investigation of concurrent energy harvesting from ambient vibrations and wind using a single piezoelectric generator, Appl. Phys. Lett. **102**, 243904 (2013)
21. M.H. Raouadi, O. Touayar, Harvesting wind energy with pyroelectric nanogenerator PNG using the vortex generator mechanism, Sens. Actuat. A **273**, 42–48 (2018)
22. A. Bakytbekov, T.Q. Nguyen, C. Huynh, K.N. Salama, A. Shamim, Fully printed 3D cube-shaped multiband fractal rectenna for ambient RF energy harvesting, Nano Energy **53**, 587-595 (2018)
23. Z. Zeng, S. Shen, X. Zhong, X. Li, Design of sub-gigahertz reconfigurable RF energy harvester from −22 to 4 dBm with 99.8% peak MPPT power efficiency, IEEE J. Solid State Circ. **54**, 2601–2613 (2019)
24. T. Umeda, H. Yoshida, S. Sekine, Y. Fujita, T. Suzuki, S. Otaka, A 950-MHz rectifier circuit for sensor network tags with 10-m distance, IEEE J. Solid State Circ. **41**, 35–41 (2006)
25. B. Li, X. Shao, N. Shahshahan, N. Goldsman, An antenna Codesign dual band RF energy harvester, IEEE Trans. Circ. Syst. I **60**, 3256–3266 (2013)
26. V. Kuhn, C. Lahuec, F. Seguin, C. Person, A multi-band stacked RF energy harvester with RF-to-DC efficiency up to 84%, IEEE Trans. Microw. Theor. Technol. **63**, 1768–1778 (2015)
27. G. Papotto, F. Carrara, A. Finocchiaro, A 90-nm CMOS 5-mbps crystal-less RF-powered transceiver for wireless sensor network nodes, IEEE J. Solid State Circ. **49**, 335–346 (2014)
28. S. Qayyum, R. Negra, 0.16 mW, 7-70 GHz distributed power detector with 75 dB voltage sensitivity in 130 Nm standard CMOS technology, in *2017 12th European Microwave Integrated Circuits Conference (EuMIC)*, Nuremberg, Germany (2017), pp. 13–16
29. M.A. Abouzied, H. Osman, V. Vaidya, An integrated concurrent multiple-input self-startup energy harvesting capacitivebased DC adder combiner, IEEE Trans. Ind. Electron. **65**, 6281–6290 (2018)
30. M. Badr, M.M. Aboudina, F.A. Hussien, Simultaneous multi-source integrated energy harvesting system for IoE applications, in *2019 IEEE 62nd International Midwest Symposium on Circuits and Systems, MWSCAS), Dallas, TX, USA* (2019), pp. 271–274
31. E.J. Carlson, K. Strunz, B.P. Otis, A 20 mV input boost converter with efficient digital control for thermoelectric energy harvesting, IEEE J. Solid State Circ. **45**, 741–750 (2010)
32. M. Wens, M. Cornelissens, K. Steyaert, A fully-integrated 0.18μm CMOS DC-DC step-up converter, using a bond wire spiral inductor, in *ESSCIRC 2007-33rd European Solid-State Circuits Conference, Munich, Germany* (2007) pp. 268–271
33. Y. Tian, L. Liu, J. Ma, A high-sensitivity, low-noise dual-band RF energy harvesting and managing system for wireless bio-potential acquisition, Microelectr. J. **116**, 105239 (2021)
34. G. Charalampidis, A. Papadakis, M. Samarakou, Power estimation of RF energy harvesters, Energy Proc. **157**, 892–900 (2019)
35. M.R. Arahal, F. Barrero, M.G. Ortega, C. Martin, Martin, Harmonic analysis of direct digital control of voltage inverters, Math. Comput. Simul. **130**, 155–166 (2016)
36. J.F. Khan, S.M.A. Bhuiyan, K.M. Rahmanb, G.V. Murphy, Space vector PWM for a two-phase VSI, Electr. Power Energy Syst. **51**, 265–277 (2013)
37. N. Onur Çetin, A.M. Hava, Topology and PWM method dependency of high frequency leakage current characteristics of voltage source inverter driven AC motor drives, 978-1-4673 −0803-8/12/$31. 00. IEEE, 2012
38. M. H. Rashid, Power Electronics Handbook (Academic Press, 2020)
39. N. Hanigovszki, J. Landkildehus, G. Spiazzi, F. Blaabjerg, An EMC evaluation of the use of unshielded MotorCables in AC adjustable speed drive applications, IEEE Trans. Power Electr. **21** (2006)
40. Z.Fang, D. Jiang, Y. Zhang, Study of the characteristics and suppression of EMI of inverter with SiC and Si devices, Chin. J. Electr Eng. **4** (2018)
41. M. Barnes, Electromagnetic compatibility (EMC), Practical Variable Speed Drives and Power Electronics, 1st Edition (2003)
42. F. Costa, C. Vollaire, Characteristics and evolution of electromagnetic noise in on-board power devices, French national committee for scientific radioelectricity, IEEE Trans. Electromagn. Compat. **50**, 445–449 (2008)
43. J. Aime, Radiation from static converters: application to the speed variation, Theses in University Joseph Fourier (2009)
44. IEC 6196 7-2, Integrated circuits − Measurement of electromagnetic emission, 150KHzto 1GHz − Part 2: Measurement of radiated emissions, TEM-cell method
45.IEC 6196 7-3, Integrated circuit − Measurement of electromagnetic emission, 150KHz to 1GHz − Part 3: Measurement of radiated emissions, surface scan method (10 kHz to3 GHz)
46. A. Boyer, S. Bendhia, E. Sicard, Characterisation of electromagnetic susceptibility of integrated circuits using near-field scan, Electron. Lett. **43**, 15–16 (2007)
47. J.Fan Near-field scanning for EM emission characterization, IEEE Electromagn. Compat. Mag. **4**, 67–73 (2015)
48. Y. Vives-Gilabert, C. Arcambal, A. Louis, Modeling magnetic radiations of electronic circuits using near-field scanning method, IEEE Trans. Electromagn. Compat. **49**, 391–400 (2007)
49. R.E. Hamam, A. Karalis, J.D. Joannopoulos, M. Soljačić, Efficient weakly-radiative wireless energy transfer: an EIT-like approach, Ann. Phys. **324**, 1783–1795 (2009)
50. K.S. Adu-Manu, N. Adam, C. Tapparello, H. Ayatollahi, Energy-Harvesting Wireless Sensor Networks (EH-WSNs): A Review, ACM Transactions on Sensor Networks **14**, 1–50 (2018)
51. F.K. Shaikh, S. Zeadally, Energy harvesting in wireless sensor networks: a comprehensive review, Renew. Sustain. Energy Rev. **55**, 1041–1054 (2016)
52. F. Gao, W. Li, X. Wang, X. Fang, M. Ma, A self-sustaining pyroelectric nanogenerator driven by water vapor, Nano Energy **22**, 19–26 (2016)
53. M. Xie, S. Dunn, E. Le Boulbar, C.R. Bowen, Pyroelectric energy harvesting for water splitting, Int. J. Hydrogen Energy 1–9 (2017)
54. Y. Zhang, P.T. Thuy Phuong, E. Roake, H. Khanbareh, Y. Wang, S. Dunn, C. Bowen, Thermal energy harvesting through pyroelectricity, Sens. Actuat. A Phys. **158**, 132–139 (2010)
55. G. Sebald, D. Guyomar, A. Agbossou, On thermoelectric and pyroelectric energy harvesting, Smart Mater. Struct. **18**, 125006 (2009)

56. M. Lallart, D. Guyomar, Y. JayetShow, R. Claude, Synchronized switch harvesting applied to self-powered smart-systems : piezo active micro-generators for autonomous wireless receiver, Sens. Actuators A Phys. **147**, 263–272 (2008)
57. U. Khaled, H. Farh, S. Alissa, A. Abanmi, O. Aldraimli, Efficient solution of the DC-link hard switching inverter of the PV system, J. King Saud Univ. Eng. Sci. **32**, 425–431 (2020)
58. M. Lallart, D. Guyomar, Y. JayetShow, R. Claude, Synchronized switch harvesting applied to self-powered smart-systems: piezo active micro-generators for autonomous wireless receiver, Sens. Actuat. A **147**, 263–272 (2008)
59. M. Tlig, J. Ben Hadj Slama, M.A. Belaid. Conducted and radiated EMI evolution of power RF N-LDMOS after accelerated ageing tests, Microelectr. Reliab. **53**, 1793–1797 (2013)

Cite this article as: Mohamed Haythem Raouadi, Jean Pierre Fanton, Oualid Touayar, First study on harvesting electromagnetic noise energy generated by the frequency converters, Int. J. Metrol. Qual. Eng. **14**, 9 (2023)